Asymptotic expressions of mismatch variance in interdigitated geometries

This is the author's version of the article that has been presented at IEEE ISCAS2020
The editorial version of the paper is available at http://dx.doi.org/10.1109/ISCAS45731.2020.9181159

Asymptotic Expressions of Mismatch Variance in Interdigitated Geometries

Carmine Paolino*, Fabio Pareschi*,‡, Riccardo Rovatti†,‡, Gianluca Setti*,‡
* DET – Politecnico of Torino, corso Duca degli Abruzzi 24, 10129 Torino, Italy.
email:{carmine.paolino, fabio.pareschi, gianluca.setti}@polito.it
† DEI – University of Bologna, viale Risorgimento 2, 40136 Bologna, Italy. email: riccardo.rovatti@unibo.it
‡ ARCES – University of Bologna, via Toffano 2/2, 40125 Bologna, Italy.

***Abstract*—Performance in analog integrated circuits strongly depends on the mismatch between nominally identical devices. In this work we derive closed-form asymptotic expressions describing mismatch variance in multifinger structures, under the assumption of Gaussian autocorrelation for the mismatch-generating stochastic process. The analysis is performed on interdigitated geometries, eventually modified to make them common-centroid. Comparison with the numerical results provided by an independent model validates the theoretical expressions presented here.**

I. Introduction

Variability in electronic devices is one of the key issues limiting performance of analog integrated circuits [1]. To get the most out of a given technological process, designers are used to adopt layout strategies allowing at least a partial compensation of this unwanted effect. Commonly accepted guidelines are based both on rules-of-thumb and analytical considerations, and typically require each device to be split into several identical segments (also knows as *fingers*) placed according to specific patterns. An example is the interdigitated layout, which alternates segments of different devices.

However, these layout strategies are often analyzed only with respect to deterministic effects such as gradients along the wafer, neglecting any stochastic variation. The well known work by Pelgrom *et al.* [2], considers random variations only in the case of adjacent devices always being uncorrelated. Under this simplifying assumption, we will actually prove that geometry does not play any role on the spreading of device parameters caused by stochastic variations.

In recent years, many works have proposed an improvement over the original Pelgrom's model for mismatch variance [3]–[6]. In [5] the hypothesis of short correlation length is removed, and in [7], the authors analyze numerically the effects of different layout strategies. The same model has been extended by Poiroux *et al.* in [6], accounting for wide sense stationary (WSS) stochastic processes whose second-order statistic (i.e., correlation) can be expressed as a linear combination of Gaussian functions. WSS processes are characterized by statistical properties that do not depend on absolute positions but are only distance-dependent.

In this paper, starting from the theoretical model in [6], we derive an approximated model of the effects of geometry on mismatch variance, under the assumption of strong device correlation. This allows us to extend the theoretical analysis conducted on pairs of devices to complex multi-finger structures, deriving closed-form expressions in the case of interdigitated layouts.

The paper is organized as follows. In Section II we will introduce the analytical model of mismatch variance on which the analysis is built, taken directly from the original paper [6] and only adapting the notation when required. In Section III we describe the geometry of interest and the approximations of the model both for extremely slow and fast decay of device correlation over distance, observing that, in the latter condition, the resulting variance is independent of the layout of the segments. In Sections IV and V we obtain simplified expression of the variance in terms of device size and placement for the multi-finger structures considered. Finally, we analyze the results in VI and then conclude the discussion.

II. Analytical Model of Mismatch Variance

Mismatch is defined as the difference in the parameters describing two nominally identical devices. It is convenient to model mismatch as a random variable, with a probability distribution that depends on its original causes. The mean of such a variable stems from deterministic effects, whereas variance is caused by random fluctuations [8]. In this work we focus on the spreading of device parameters due to the latter effect. Since a large spreading might result in circuits not satisfying their design specifications, hence limiting the yield, quantifying variance becomes of paramount importance. The analysis proposed here is based on the results obtained in [6], and relies on the following assumptions.

Let us consider two nominally identical devices occupying rectangular regions A and B on the Euclidean plane with Cartesian coordinates (x, y) as schematized in Figure 1(a). Both devices are characterized by dimensions D_x and D_y, and their centroids are separated by distances P_x and P_y. The lowercase names appearing in the figure refer to these dimensions normalized by a suitable parameter introduced later in this section. We investigate the variation of a device parameter p that is defined pointwise on the euclidean plane by means of the WSS process $p(x, y)$. The actual value of the parameter for the two structures is indicated with $\bar{p}_A$ and $\bar{p}_B$, and is computed as the average value $\bar{p}$ of the process $p(x, y)$ over the area occupied by the two devices. Let finally be $\langle p \rangle$ the average value of $p(x, y)$ over the entire area of interest (i.e., the whole die, or the region where the structure is placed).

The original model in [6] represents processes $p(x, y)$ defined by means of a linear combination of Gaussian au-

This is the author's version of the article that has been presented at IEEE ISCAS2020
The editorial version of the paper is available at http://dx.doi.org/10.1109/ISCAS45731.2020.9181159

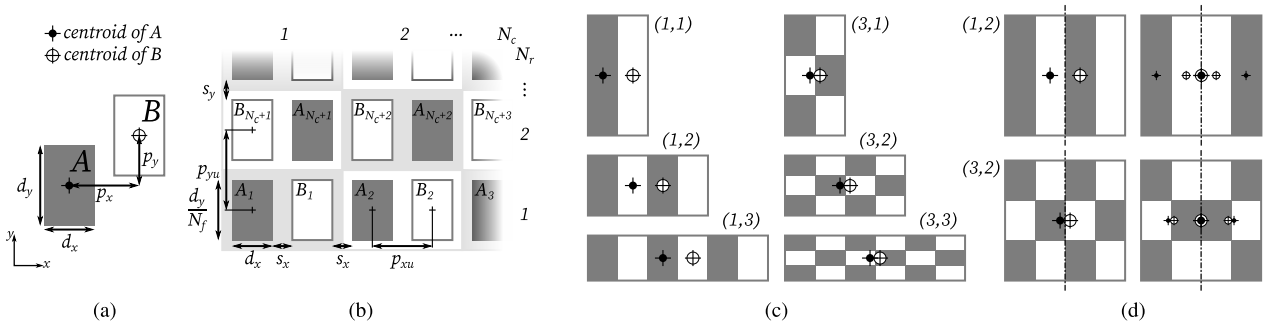

Fig. 1. (a) Geometry of devices A and B. (b) Interdigitated layout on a grid of N_r rows and N_c columns. Device segments are named linearly, starting from the bottom left corner. (c) Invariance of centroid distance on the number of columns N_c for a given number of rows N_r (negligible spacing between segments). In parenthesis, the couple (N_r, N_c) for each layout. (d) Mirroring half of the array to obtain a common centroid structure for N_c even and N_r odd. The centroids of the half arrays are also highlighted in the mirrored structures.

tocorrelations, here we will limit our analysis to a single multivariate normal component, with independent x and y contributions. This assumption allows us to mathematically define the correlation lengths Λ_x and Λ_y along the two plane directions as $\sqrt{2}\sigma_x$ and $\sqrt{2}\sigma_y$, respectively, with σ_x and σ_y being the standard deviations of the Gaussian functions under consideration.

Instead of the actual values of D_x, D_y, P_x and P_y, it is convenient to handle their dimensionless counterparts d_x, d_y, p_x, and p_y, obtained after a normalization by Λ_x or Λ_y. Employing this notation, the main result of [6] is to express, for A and B, the autocorrelation of the difference $\bar{p} - \langle p \rangle$ as

$$\Gamma_{\bar{p}-\langle p\rangle}(p_x, p_y) = \frac{\alpha}{4 d_x^2 d_y^2 \Lambda_x \Lambda_y} \gamma(p_x, d_x)\gamma(p_y, d_y), \quad (1)$$

where α is a scaling parameter expressed in the appropriate units, and the remaining dimensionless factors are

$$\gamma(p, d) = \theta(p + d) - 2\theta(p) + \theta(p - d),$$

being

$$\theta(u) = u \times \mathrm{erf}(u) + e^{-u^2}/\sqrt{\pi}.$$

The variance of $\Delta\bar{p} = \bar{p}_A - \bar{p}_B$, representing the spread of the difference between the parameters describing devices A and B, can then be expressed as

$$\sigma^2_{\Delta\bar{p}} = 2\left[\Gamma_{\bar{p}-\langle p\rangle}(0, 0) - \Gamma_{\bar{p}-\langle p\rangle}(p_x, p_y)\right]. \quad (2)$$

Table 1 in the original work [6] collected asymptotic approximations for this formula under the limiting conditions of p_x, p_y, d_x and d_y. In the following, this procedure will be extended to multi-finger devices placed on a generic 2D grid.

III. Geometry and Model Approximation

Consider a 2D grid of N_r rows and N_c columns. The original devices A and B, with physical dimensions $D_y = W$ and $D_x = L$, are divided into $N_f = N_r N_c$ segments each, preserving the total area. The segment length is assumed to be the same of the original device L, hence the height has to be scaled by $1/N_f$. Each grid cell contains one segment of A and one of B, as depicted in Figure 1(b), so that segments of different devices alternate on the plane (interdigitation), separated by distances S_x and S_y. Given the extension of the grid, the size of the devices, and the spacing between their segments, our goal is to obtain an approximation of the mismatch variance simple enough to be used for paper-and-pencil calculations.

The generalization of (2) to multi-finger structures is:

$$\sigma^2_{\Delta\bar{p}} = \frac{2}{N_f^2}\sum_{i=1}^{N_f}\sum_{j=1}^{N_f}\Big[\,\Gamma_{\bar{p}-\langle p\rangle}\left(p_x^{AA}(i,j), p_y^{AA}(i,j)\right) - \Gamma_{\bar{p}-\langle p\rangle}\left(p_x^{AB}(i,j), p_y^{AB}(i,j)\right)\Big], \quad (3)$$

where i and j are linear indices defined on the grid (e.g. starting from the bottom-left corner with segments A_1 and B_1 as in Figure 1(b)) and $p_x^{AA}(i,j)$ is the distance between segments i and j of device A, while $p_x^{AB}(i,j)$ is computed between segment i of device A and segment j of device B. Similar definitions stand for $p_y^{AA}(i,j)$ and $p_y^{AB}(i,j)$. Closed-form expressions for the double summation can be obtained for asymptotic values of the normalized dimension, as shown in the following.

A. Small correlation lengths ($d_x, d_y, p_x, p_y \gg 1$)

Under the assumption of small correlation lengths, normalized sizes and distances assume values much greater than 1, therefore we can express $\theta(u)$ as

$$\theta(u) \simeq \begin{cases} |u| & \text{if } u \neq 0 \\ \dfrac{1}{\sqrt{\pi}} & \text{if } u = 0\,. \end{cases} \quad (4)$$

The term for $u = 0$ is necessary since, whenever in (3) we have $i = j$, i.e. we consider the couple made of a segment of A and itself, the distance terms $p_x^{AA}(i,j)$ and $p_y^{AA}(i,j)$, which are arguments of θ, are equal to 0 no matter the correlation lengths.

Assuming $d \neq 0$, $p \geq 0$ and $p > d$ whenever $p \neq 0$, then

$$\gamma(p, d) \simeq \begin{cases} 2d - \dfrac{2}{\sqrt{\pi}} \simeq 2d & \text{if } p = 0 \\ 0 & \text{otherwise.} \end{cases}$$

Hence the autocorrelation of $\bar{p} - \langle p \rangle$ becomes

$$\Gamma_{\bar{p}-\langle p\rangle}(p_x, p_y) \simeq \begin{cases} \dfrac{\alpha}{d_x d_y \Lambda_x \Lambda_y} & \text{if } p_x = p_y = 0 \\ 0 & \text{otherwise}\,. \end{cases}$$

This is the author's version of the article that has been presented at IEEE ISCAS2020
The editorial version of the paper is available at http://dx.doi.org/10.1109/ISCAS45731.2020.9181159

Plugging this expression into (3) and considering that $p_x^{AB}(i,j)$ and $p_y^{AB}(i,j)$ are always nonzero, we obtain

$$\begin{aligned}\sigma^2_{\Delta\bar{p}} &\simeq \frac{2}{N_f^2}\sum_{i=1}^{N_f}\sum_{j=1}^{N_f}\Gamma_{\bar{p}-\langle p\rangle}\left(p_x^{AA}(i,j), p_y^{AA}(i,j)\right)\\ &= \frac{2}{N_f^2}\sum_{i=1}^{N_f}\left(\sum_{j\neq i}0 + \Gamma_{\bar{p}-\langle p\rangle}(0,0)\right)\\ &= \frac{2\alpha}{\Lambda_y\Lambda_x}\frac{1}{wl} = \frac{2\alpha}{WL}.\end{aligned}$$

This result corresponds to the traditional model derived by Pelgrom in [2], where variance depends on the inverse of device area. The expression depends neither on the position of the fingers nor on their number hence, under the assumption of correlation lengths much shorter than device sizes, geometry has no effect on the variance whatsoever.

B. Large correlation lengths ($d_x, d_y, p_x, p_y \ll 1$)

Large correlation lengths result in normalized device sizes and distances tending towards 0. The asymptotic approximation of (1) under this assumption is trivial. Its expression is not included here for compactness reasons, but will be used in the following sections to derive our main results.

In any case the linear indexing method employed in (3) is not convenient when working on a 2D grid since the expressions of the distance terms ($p_x^{AA}(i,j)$ and the others) become unmanageable. Indexing the segments through their row and column indices we can write, equivalently:

$$\begin{aligned}\sigma^2_{\Delta\bar{p}} = \frac{2}{N_r^2N_c^2}&\sum_{r_i=1}^{N_r}\sum_{c_i=1}^{N_c}\sum_{r_j=1}^{N_r}\sum_{c_j=1}^{N_c}\\ &\left[\,\Gamma_{\bar{p}-\langle p\rangle}(p_x^{AA}(r_i,c_i,r_j,c_j), p_y^{AA}(r_i,c_i,r_j,c_j))\right.\\ &\left.-\,\Gamma_{\bar{p}-\langle p\rangle}(p_x^{AB}(r_i,c_i,r_j,c_j), p_y^{AB}(r_i,c_i,r_j,c_j))\right]. \quad (5)\end{aligned}$$

In general, (5) can be used to compute the variance for any 2D grid-based geometry, once the distance terms have been determined. For simplicity, the notation will be simplified in the following by not writing the explicit dependence of distances on the row and column indices.

IV. Variance in Interdigitated Structures

In an interdigitated layout as the one depicted in Figure 1(b), segment distances can be expressed as:

$$\begin{aligned}p_x^{AA} &= p_{xu}\,|2(c_i-c_j) + \mathbf{1}_{\mathrm{odd}}(r_i+r_j)|\\ p_x^{AB} &= p_{xu}\,|2(c_i-c_j) + \mathbf{1}_{\mathrm{even}}(r_i+r_j)|\\ p_y^{AA} &= p_{yu}\,|r_i-r_j|\\ p_y^{AB} &= p_{yu}\,|r_i-r_j|\,,\end{aligned} \quad (6)$$

where $p_{xu} = l + s_x$ and $p_{yu} = w/N_f + s_y$ are the distances between adjacent segments. The indicator function $\mathbf{1}_A(n)$ checks the membership of its argument to the set S and is defined as:

$$\mathbf{1}_S(x) = \begin{cases}1 & \text{if } x \in S\\ 0 & \text{otherwise}\,.\end{cases}$$

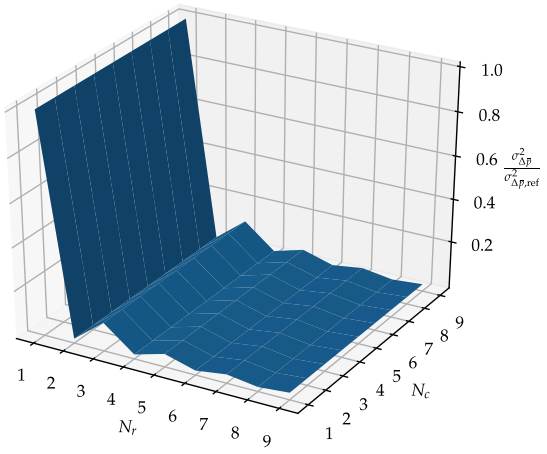

Fig. 2. Mismatch variance computed through (7) and normalized to the value obtained for $N_r = N_c = 1$. ($w = 0.02$, $l = 0.001$)

It is employed in this context to account for the alternation of segment positions across consecutive rows of the grid. In the specific case of $\mathbf{1}_{\mathrm{odd}}(n)$, the function evaluates to 1 whenever n is odd. Equivalently for $\mathbf{1}_{\mathrm{even}}(n) = 1 - \mathbf{1}_{\mathrm{odd}}(n)$. An expression for $\mathbf{1}_{\mathrm{odd}}(n)$ that is also suitable for symbolic manipulation is given by

$$\mathbf{1}_{\mathrm{odd}}(n) = \frac{1-(-1)^n}{2}.$$

Combining expressions (6) and (5), and using Taylor's expansion of (1) around 0 (because of the large correlation lengths), mismatch variance can be expressed as:

$$\begin{aligned}\sigma^2_{\Delta\bar{p}} &\simeq \frac{2\alpha}{\pi\Lambda_x\Lambda_y}p_{xu}^2\left(\frac{1}{N_r^2}\mathbf{1}_{\mathrm{odd}}(N_r) + \frac{p_{yu}^2}{2}\mathbf{1}_{\mathrm{even}}(N_r)\right)\\ &= \begin{cases}\dfrac{2\alpha}{\pi\Lambda_x\Lambda_y}\dfrac{p_{xu}^2}{N_r^2} & \text{if } N_r \text{ odd}\\ \dfrac{2\alpha}{\pi\Lambda_x\Lambda_y}\dfrac{p_{xu}^2p_{yu}^2}{2} & \text{if } N_r \text{ even}\,.\end{cases}\end{aligned} \quad (7)$$

The dependence on geometry is explicit in the term N_r^{-2} and is also embedded in the value of p_{yu}. If the device segments are tightly spaced, i.e. $s_x = s_y \approx 0$, (7) reduces to

$$\sigma^2_{\Delta\bar{p}} \simeq \begin{cases}\dfrac{2\alpha}{\pi\Lambda_x\Lambda_y}\dfrac{l^2}{N_r^2} & \text{if } N_r \text{ odd}\\ \dfrac{2\alpha}{\pi\Lambda_x\Lambda_y}\dfrac{l^2w^2}{2N_r^2N_c^2} & \text{if } N_r \text{ even}\end{cases} \quad (8)$$

which is depicted in Figure 2 with respect to $\sigma^2_{\Delta\bar{p},\mathrm{ref}}$, evaluated for ($N_r$, N_c) = (1, 1). The plot highlights the constant-valued peaks whenever the number of rows is odd, notwithstanding the fact that as the number of columns grows, the increasingly smaller device segments are more uniformly spread in the grid area. The valleys in the plot actually vary with N_c, but it is not apparent in linear scale.

Intuitively, increasing N_c changes the absolute positions of the centroids of A and B with respect to the origin of the grid, as shown in Figure 1(c), although their relative distance

This is the author's version of the article that has been presented at IEEE ISCAS2020
The editorial version of the paper is available at http://dx.doi.org/10.1109/ISCAS45731.2020.9181159

is unaffected. Since N_r odd implies a non-common-centroid geometry, the constant centroid distance results in a constant contribution to the variance. Increasing the number of rows to a larger odd number, such a distance decreases, but is still invariant with respect to N_c. Conversely, whenever N_r is even the centroids of A and B coincide and higher order effects result in N_c actually having an effect on the variance.

V. Variance in a Mirrored Interdigitated Layout

As already pointed out, the simple interdigitated layout in Figure 1(b) is not common centroid whenever the number of rows is odd. If, at the same time, the number of columns is even, it is actually possible to obtain a common centroid geometry simply by mirroring the right half of the structure, as shown in Figure 1(d). The expressions of segment distances describing such a layout require the introduction of the sets $L = \{1, \ldots, N_c/2\}$ and $R = \{N_c/2+1, \ldots, N_c\}$, which characterize the columns as belonging either to the left (straight) or the right (mirrored) half of the array. Thus we can write:

$$\begin{aligned} p_x^{AA} = p_{xu} \,|&2\,(c_i - c_j) \\ &+\mathbf{1}_{\text{odd}}(r_i + r_j)\,[\mathbf{1}_{\text{L}}(c_i)\mathbf{1}_{\text{L}}(c_j) - \mathbf{1}_{\text{R}}(c_i)\mathbf{1}_{\text{R}}(c_j)] \\ &+\mathbf{1}_{\text{even}}(r_i)\mathbf{1}_{\text{even}}(r_j)\mathbf{1}_{\text{L}}(c_i)\mathbf{1}_{\text{R}}(c_j) \\ &+\mathbf{1}_{\text{odd}}(r_i)\mathbf{1}_{\text{odd}}(r_j)\mathbf{1}_{\text{R}}(c_i)\mathbf{1}_{\text{L}}(c_j)| \\ p_x^{AB} = p_{xu} \,|&2\,(c_i - c_j) \\ &+\mathbf{1}_{\text{even}}(r_i + r_j)\,[\mathbf{1}_{\text{L}}(c_i)\mathbf{1}_{\text{L}}(c_j) - \mathbf{1}_{\text{R}}(c_i)\mathbf{1}_{\text{R}}(c_j)] \\ &+\mathbf{1}_{\text{even}}(r_i)\mathbf{1}_{\text{odd}}(r_j)\mathbf{1}_{\text{L}}(c_i)\mathbf{1}_{\text{R}}(c_j) \\ &+\mathbf{1}_{\text{odd}}(r_i)\mathbf{1}_{\text{even}}(r_j)\mathbf{1}_{\text{R}}(c_i)\mathbf{1}_{\text{L}}(c_j)|\,. \end{aligned}$$

Distances along y are unchanged with respect to (6).

Following the same procedure as in the previous section, the variance can be expressed as:

$$\sigma^2_{\Delta\bar{p}} \simeq \frac{2\alpha}{\pi\Lambda_x\Lambda_y}\frac{3}{2}\left(\frac{N_c}{N_r}\right)^2 p_{xu}^4 \qquad \begin{matrix}\text{if } N_r \text{ odd} \\ \text{and } N_c \text{ even}\end{matrix} \tag{9}$$

Being p_{xu} a constant, the dependence on the geometry is determined only by the ratio $(N_c/N_r)^2$. Intuitively, as N_r is increased, the centroids in each half of the array get closer, increasing the correlation between the devices and thus reducing the variance. Conversely, as N_c increases, the distance between the centers of the two halves of the array grows, resulting in a larger variance.

VI. Results

Figure 3 shows the normalized behaviour of variance for the layouts analyzed in this work. The results from the approximate models (7) and (9) are compared to the variance computed on 10000 Monte Carlo trials of the CAD-friendly model developed by Lu in [9] and analyzed also in [6]. The maximum relative error between datapoints in Figure 3 is less than 2%, validating the approximate expressions. For the sake of clarity, the geometries corresponding to some of the data points have been superimposed to the plot. In particular they represent the structures forced to be common centroid, highligting the reduction in variance obtained by such a modification.

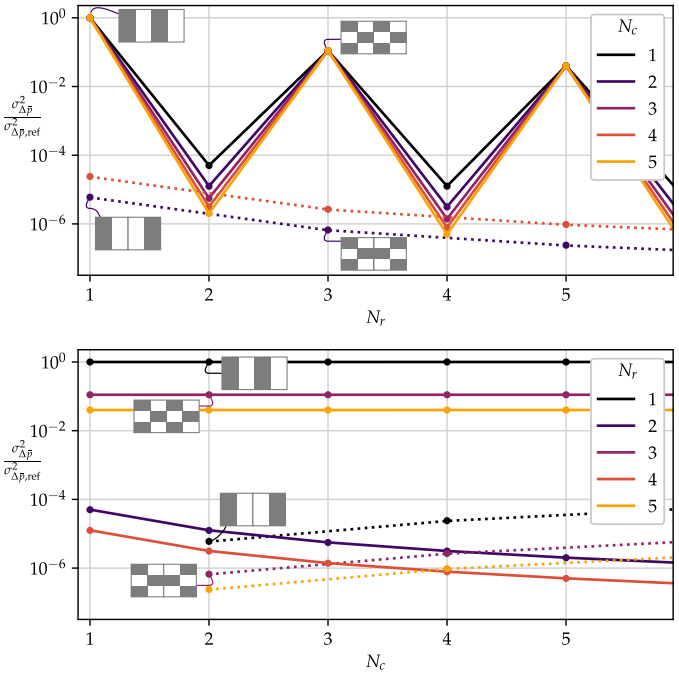

Fig. 3. Mismatch variance normalized with respect to the value for $N_r = N_c = 1$. Lines are obtained through a Monte Carlo simulation using the model in [9], markers using the asymptotic expressions derived in this work. Solid lines refer to the simple interdigitated layout, dotted lines to the mirrored geometry. ($w = 0.02$, $l = 0.001$, $s_x = s_y = 0$, $\Lambda_x = \Lambda_y = 10^3$, $\alpha = 1$)

In Table I we have computed the asymptotic expressions derived in this work for two-fingers geometries, normalized with respect to the variance $\sigma^2_{\Delta\bar{p},\text{ref}}$ of the reference, single-finger layout ($N_r = N_c = 1$). With negligible device spacing, the cross-coupled layout performs better than the mirrored-linear one whenever $(w/l)^2 < 12$.

TABLE I
Mismatch variance for two-finger layouts, with respect to the single-finger reference case $(N_r, N_c) = (1, 1)$.

(1,2) linear	(1,2) half-mirrored linear	(2,1) cross-coupled
$\sigma^2_{\Delta\bar{p},\text{ref}}$	$\frac{3}{2}(l + s_x)^2\,\sigma^2_{\Delta\bar{p},\text{ref}}$	$\frac{1}{2}\left(\frac{w}{2} + s_y\right)^2\sigma^2_{\Delta\bar{p},\text{ref}}$

VII. Conclusion

We have shown that under the assumption of correlation lengths much shorter than device sizes geometry does not play any role in reducing the variance of parameter mismatch. Conversely, when correlation lengths are long, we have obtained closed-form expressions linking variance to the parameters of the interdigitated geometry. The results have been compared to an independent model, showing extremely good agreement, thus validating our derivation.

References

[1] D. M. Binkley, *Tradeoffs and optimization in analog CMOS design*. Chichester, England; Hoboken, NJ: John Wiley & Sons, 2008.

[2] M. Pelgrom, A. Duinmaijer, and A. Welbers, "Matching properties of MOS transistors," *IEEE Journal of Solid-State Circuits*, vol. 24, no. 5, pp. 1433–1439, Oct. 1989.

[3] J. A. Croon, W. M. C. Sansen, and H. E. Maes, *Matching properties of deep sub-micron MOS transistors*, ser. The Kluwer international series in engineering and computer science. New York: Springer, 2005, no. 851.

[4] D. Reid, C. Millar, S. Roy, and A. Asenov, "Understanding LER-Induced MOSFET V_{T} VariabilityPart I: Three-Dimensional Simulation of Large Statistical Samples," *IEEE Transactions on Electron Devices*, vol. 57, no. 11, pp. 2801–2807, Nov. 2010.

[5] M. Conti, P. Crippa, S. Orcioni, and C. Turchetti, "Parametric yield formulation of MOS IC's affected by mismatch effect," *IEEE Transactions on Computer-Aided Design of Integrated Circuits and Systems*, vol. 18, no. 5, pp. 582–596, May 1999.

[6] T. Poiroux, P. Scheer, A. Juge, and M. Vinet, "Multiscale statistically correlated variability: A unified model for computer-aided design," *IEEE Transactions on Electron Devices*, vol. 62, no. 11, pp. 3605–3612, Nov. 2015.

[7] M. Conti, P. Crippa, S. Orcioni, and C. Turchetti, "Layout-based statistical modeling for the prediction of the matching properties of MOS transistors," *IEEE Transactions on Circuits and Systems I: Fundamental Theory and Applications*, vol. 49, no. 5, pp. 680–685, May 2002.

[8] A. Hastings, *The art of analog layout*, 2nd ed. Upper Saddle River, NJ: Pearson/Prentice Hall, 2006.

[9] N. Lu, "Modeling of Distance-Dependent Mismatch and Across-Chip Variations in Semiconductor Devices," *IEEE Transactions on Electron Devices*, vol. 61, no. 2, pp. 342–350, Feb. 2014.